Int. J. Electrochem. Sci., 16 **(2021)** Article Number: 211239, doi: 10.20964/2021.12.28

International Journal of
ELECTROCHEMICAL
SCIENCE
www.electrochemsci.org

Effect of polyaniline and aluminum tri-polyphosphate particles addition on the protective properties of Mg-rich epoxy coating on AZ91D magnesium alloy

Xiangyu Lu[1#], Xiao Wang[2#], Song Chen[1], Jiatao Cai[1], Hong Tao[1], Zhikai Xu[1], Xingguo Feng[1]*

[1] Key Laboratory of Coastal Disaster and Defence (Hohai University), Ministry of Education, Nanjing 210024 Jiangsu, China
[2] Marine Chemical Research Institute, State Key Laboratory of Marine Coatings, Qingdao, 266072, China
Xiangyu Lu and Xiao Wang are co-first authors of the article.
*E-mail: fengxingguo@hhu.edu.cn

Received: 6 September 2021 / *Accepted:* 8 October 2021 / *Published:* 10 November 2021

Hydrofluoric acid doped PANI (PANI-HF) and aluminum tri-polyphosphate (SAP) particles were together added into a Mg-rich primer (MRP) on the AZ91D magnesium alloy and improved the protective performance of the MRP greatly. The coating performance was studied with Machu test, OCP and EIS. The surface analysis was conducted on the coating and the AZ91D substrate using SEM and XPS. The results showed that the protective effect of the PANI-HF/SAP/MRP was better than that of the MRP for the substrate underneath the defect coating. On one hand, the corrosion products, consisting of magnesium oxides and phosphates, precipitated on the Mg particles, which healed the micro defects in the coating and improved its barrier effects. On the other hand, a protective film was formed on the AZ91D substrate, which could prevent the permeation of the electrolyte and retard the corrosion of the substrate.

Keywords: Magnesium alloy; Mg-rich epoxy coating; Polyaniline; Aluminum Tri-polyphosphate; EIS

1. INTRODUCTION

Magnesium alloys have an extensive application prospect in aviation, aerospace and automobile industries due to their advantages of low densities, excellent castability and high specific strength [1, 2]. Nevertheless, the poor corrosion resistance is one of the biggest obstacles to the widespread adoption of Mg alloys. Hence improving the corrosion resistance of magnesium alloys through surface engineering is one of the hot topics in the research of magnesium alloys [3-5]. Compared with other anti-corrosion technologies, organic coatings have low cost, simple process and

excellent anti-corrosion performance and are widely used in the magnesium alloy protection [6, 7]. However, damage and cracking of organic coatings inevitably occur due to the environmental aging or external force damage in the process of a long-term service, resulting in the substrate corrosion at defects and accelerated the coating failure [8]. Therefore, it is necessary to improve the damage resistance of the coating, reduce the adverse effect of the coating defect on its protection performance, and construct a self-healing long-acting coating system on the surface of Mg alloys.

In recent years, a Mg-rich primer (MRP) has been developed to provide the cathodic protection to AZ91D Mg alloys [9, 10]. It was verified by Song et al. that the corrosion rate of Mg alloys decreased significantly when the cathodic polarization reached ~ 30 mV [11]. In addition, the corrosion potentials of Mg alloys are usually higher than that of a pure Mg because Mg alloys contain alloying elements such as Al, Zn and so on [12]. Therefore, pure Mg particles were added into the epoxy coatings to develop MRPs in order to provide the cathodic protection for the AZ91D alloy [9, 10, 13-16]. Pure Mg particles could provide the cathodic protection for the AZ91D alloy, strengthening the protective properties of epoxy coatings [9, 10]. A three-stage mechanism was proposed to illustrate the protection of MRPs to the AZ91D alloy [10]. In the first place, the AZ91D substrate is protected by the barrier effect of MRPs; at the same time, the Mg particles in MRPs are gradually activated by the permeated water. In the second place, Mg particles provide the cathodic protection to the AZ91D alloy via their anodic dissolution. In the end, the barrier effect of MRPs is improved to some extent by the precipitation of $Mg(OH)_2$. Nevertheless, the extreme reactivity of Mg particles causes $Mg(OH)_2$ to accumulate in MRPs quickly, resulting in that the cathodic protection failed rapid [9, 10]. In addition, due to the relatively loose structure of $Mg(OH)_2$, the improvement effect of Mg particles on MRPs for AZ91D alloy is not so good as that of Zn powders on Zn-rich primers for steels [9, 10, 14-18]. Therefore, on the basis of ensuring the cathodic protection effect of pure Mg particles on Mg alloys, it is the key to prolong the life of a MRP that appropriately reducing the activity of Mg particles and enhancing the compactness of their corrosion products.

The measures of improving performance of the MRPs on Al alloys or Mg alloys can fall into two categories. One method is to coat pure Mg particles to reduce their initial reaction rate [19-21]. Pathak et al. carbonized Mg particles to coat them with Mg carbonate and found that the carbonization treated Mg particles could provide good protection to A2024 aluminum alloy compared with the untreated Mg particles [19]. Wang et al. adopted a dilute phosphoric acid to pretreat Mg particles, leading to the formation of Mg phosphate on their surfaces [20]. It was reported that the phosphatized Mg particles could strengthen the barrier effect of MRPs on Al alloys in initial stage and the phosphate ions released by Mg phosphate could retard the substrate corrosion in the late stage [20]. A stannate bath was used by Xu et al. to pretreat Mg particles and Mg stannate was successfully coated on their surfaces [21]. The stannate treatment could retard the dissolution rate of Mg particles and generated a protective film on the AZ91D alloy, prolonging the protective life of the MRP [21]. In general, the reaction activity of Mg particles can be effectively retarded by coating corrosion inhibition film on their surfaces, but the coating process is relatively complicated.

The other method is adding corrosion inhibiting particles directly to MRPs, developing a long-acting protective MRP. Lu et al. [14, 22] found that the aluminum tri-polyphosphate (SAP) pigment can significantly prolong the protective performance of MRPs and revealed the mechanism of SAP:

firstly, SAP can prolong the cathodic protection period of pure Mg particles in MRPs; secondly, SAP densifies the corrosion products of Mg particles, improving the barrier effect of MRPs; Finally, the reaction between the SAP and the AZ91D alloy generates a protective film on the AZ91D alloy, further improving the protective performance of MRPs. Shen et al. added ZnO particles into MRPs and found that they could decrease the corrosion rate of Mg particles and improve the physical crosslink density of the epoxy matrix, resulting in the enhancement of the barrier effect and adhesion for MRPs on the AZ91D substrate [23]. Shen et al. also added 8-hydroxyquinoline (8-HQ) to MRPs and found that 8-HQ combined with Mg^{2+} to form MgQ_2, which could retard dissolution of Mg particles, block the defects in MRPs and inhibit active sites on the AZ91D alloy [24]. Feng et al. added hydrofluoric acid doped polyaniline (PANI-HF) particles into MRPs to improve their protective performance on the AZ91D alloy [25]. The improvement effect of PANI-HF particles on MRPs could be divided into the following aspects [25]: firstly, the cathodic protection was enhanced by the improvement of the electrical contact between Mg particles and the AZ91D alloy; next, the corrosion products, MgO and MgF_2, accumulated around Mg particles in MRPs, improving their barrier effects; meanwhile, some chloride ions were captured by PANI, which retard the degradation of MRPs; finally, the corrosion of the AZ91D alloy were reduced by the formation of a protective layer between MRPs and the substrate. To date, all the studies of the MRP improvement by adding corrosion inhibitor particles have focused on the addition of one particle and the synergistic improvement effect of more than two kinds of particles has not been studied. In this work, both PANI-HF particles and SAP pigment were added into MRPs in order to construct a self-healing long-acting coating on the surface of AZ91D alloys.

2. EXPERIMENTAL METHODS

2.1. Materials

AZ91D alloys were purchased from Yingkou galaxy magnesium aluminum Co., Ltd, China. The chemical compositions were displayed in Table 1.

A two-component commercial epoxy varnish primer (KFH-01) was employed in this study and supplied by Shijiazhuang Golden Fish Paint Company, China. The purity of Mg particles was 99.9% and their average diameter size is 5–10 μm. The Mg particles were provided by Tangshan Weihao Magnesium Powder Co., Ltd, Tangshan Hebei, China. Jinhong Rubber Industry Co., Ltd, China supplied the γ-glycidoxy propyl trimethoxy silane (γ-GPS) coupling agent. Emeraldine base PANI was obtained from Cool Chemical Technology (Beijing) co. Ltd, China. Hydrofluoric acid doped PANI (PANI-HF) were prepared using a method according to a procedure we reported earlier [25]: 0.2 L of 2 mol L^{-1} hydrofluoric acid solution was used to disperse some of the PANI particles; mix with agitation for ~0.5 h and allow the solution to stand for 24 h at ambient temperature; the particles were filtered and dried at 45 ℃ for 48 h in a vacuum oven to obtain PANI-HF. The aluminum tri-polyphosphate was commercial grade modified pigment and obtained from Shanghai Yipin Pigments Co., Ltd., China. SAP was used to call the modified aluminum tri-polyphosphate in the following.

Table 1. Nominal composition (wt.%) of AZ91D alloy

Al	Zn	Mn	Si	Fe	Ni	Cu	Mg
9.4	0.82	0.23	0.01	0.005	0.002	0.02	remainder

2.2. Sample preparation

The commercial AZ91D alloy sheets were cut into small samples with dimensions of 50 mm × 50 mm × 3 mm. The AZ91D samples were polished to 240 grit by a water abrasive paper. Then the substrate samples were washed with deionized water, degreased with ethanol and acetone, and finally dried with cold air.

Different MRPs were prepared by adding pure Mg particles, PANI-HF particles or SAP pigments into the epoxy primer. The MRP with PANI-HF and SAP was labeled as PANI-HF/SAP/MRP. The dispersing agent was γ-GPS coupling agent and its amount added in the coating was 1% w/w with respect to the pigment mass. The dispersion of pigments in epoxy component of coating was conducted with a high speed agitation equipment. After stirring for 10 min, the polyamide hardener (3:10 with respect to the epoxy component weight) was added to the coating. The coated samples were prepared by manual brushing. Before being tested, the samples were dried indoors for 7 days. A coating thickness gauge (EC776FN) was employed to measure the coating thickness which was ~ 130 μm (±10 μm).

2.3. Characterization techniques

Machu test was carried out in order to evaluate the protective performance of different coatings on the AZ91D alloys at the coating defects. Prior to Machu test, the coated samples were scribed on the surface with a razor blade and then their edges were sealed with HY-914 resin. The samples were immersed in a solution of 5% NaCl, 10% H_2O_2 and 10 ml/L acetic acid at 37 ℃ for 48 h. After 24 h of exposure, another 10% H_2O_2 was supplemented in the test solution. A digital camera was used to record the coating morphology and the corrosion phenomena on the AZ91D substrate.

An electrochemical workstation (Metrohm, AutoLab 302N, Switzerland) was employed to conduct electrochemical impedance spectroscopy (EIS) experiments in 3 wt.% NaCl solution. Both intact coatings and defected coatings were tested in the frequency range of 100 kHz to 10 mHz, and AC signal with a sinusoidal amplitude of 10 mV around open circuit potentials (OCP). A hole deep into the substrate was made on the coating with a steel needle in order to prepare defected samples. The reference electrode was a saturated calomel electrode (SCE) and the counter electrode was a Pt mesh. The working area of intact samples was 10 cm^2. The EIS results were fitted with ZSimpWin software. The OCPs of different samples were measured before the EIS measurement. At least 3 parallel samples were tested in the electrochemical measurements to ensure the reproducibility.

Scanning electron microscope (SEM) analysis via a Hitachi S4700 was conducted to investigate the morphology of the defected coatings and the film on the AZ91D surface. The samples were sprayed with gold before analyzed.

X-ray photoelectron spectroscopy (XPS) was carried out to analyze the surface compositions of the AZ91D substrate underneath the PANI-HF/SAP/MRP with an ESCALAB 250 instrument, with a monochromatized Al K line (1486 eV) as the excitation source. C 1 s peak at 284.6 eV was utilized to calibrate all the binding energy values. The fitting results of the narrow scan spectra were obtained with XPSPEAK 4.1 software.

3. RESULTS AND DISCUSSION

3.1. Machu test

Figure 1 revealed the corrosion morphology of the MRP and PANI-HF/SAP/MRP coated samples after the Machu test. Severe coating delamination occurred along the scratches of the MRP coated sample (Fig. 1a). After the MRP was removed from the alloy, the substrate morphology exhibited severe corrosion damage (Fig. 1b). In contrast, the coating of the PANI-HF/SAP/MRP remained good adhesion without serious disbanding (Fig. 1c) and the corrosion extent of the substrate (Fig. 1d) was lighter than that of the substrate underneath the MRP, indicating that the protective properties of the MRP on the AZ91D alloy were obviously improved by the SAP pigments and the PANI-HF particles.

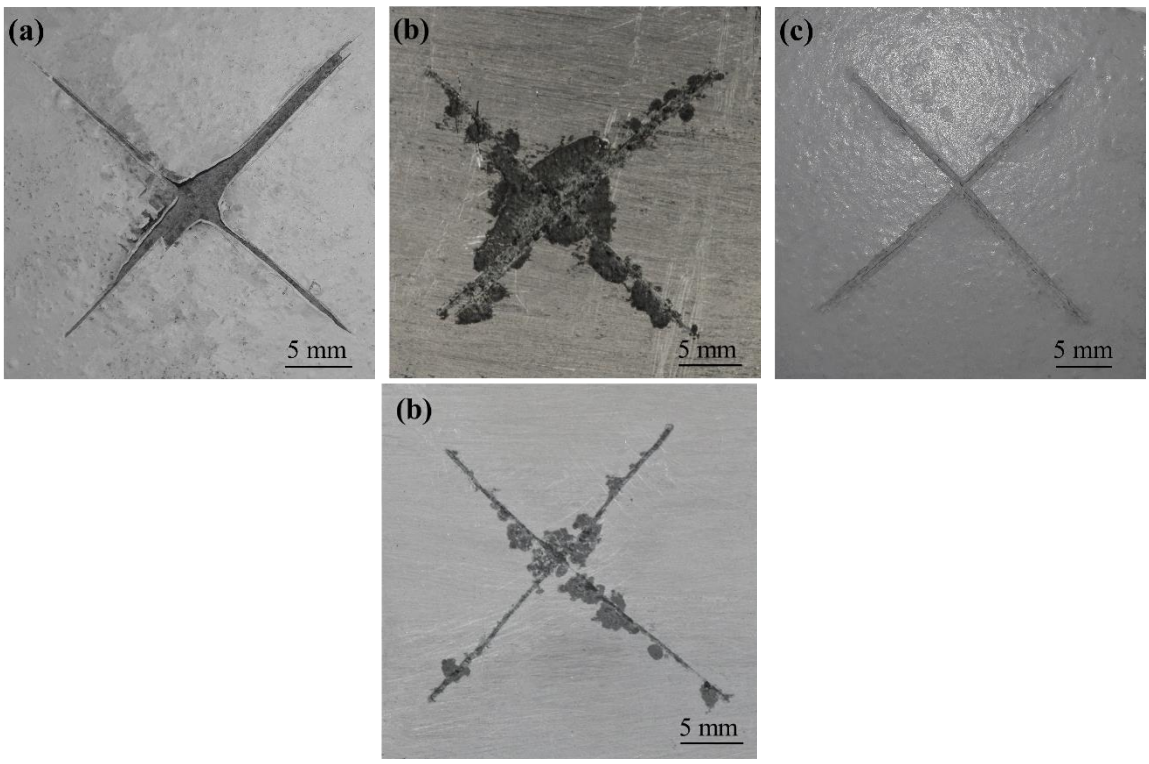

Figure 1. Machu test results of scratched samples: (a) MRP; (b) MRP, coating removed; (c) PANI-HF/SAP/MRP; (d) PANI-HF/SAP/MRP, coating removed.

3.3. OCP

Figure 2 presented the variations of the OCPs for the MRP and PANI-HF/SAP/MRP coated samples in the 3 wt% NaCl solution. Our previous studies demonstrated that the E_{OCP} for the bare AZ91D alloy was ~-1.5 V_{SCE} in the 3 wt% NaCl solution [9]. Therefore, the coating can provide the cathodic protection for the AZ91D alloy if the E_{OCP} value of the coating sample is lower than -1.5 V_{SCE}. In the initial immersion, the E_{OCP} value of the MRP coted sample was below -1.5 V_{SCE}, suggesting that the AZ91D alloy underneath the MRP was cathodically protected. With immersion time prolonging, the E_{OCP} value of the MRP sample increased because of the precipitation of $Mg(OH)_2$ around Mg particles [9]. the E_{OCP} value was above -1.5 V_{SCE} after 5 days of immersion, indicating that the cathodic protection failed. After about 70 days of immersion, the E_{OCP} value declined gradually to the active direction. Finally, after 98 days of immersion, the E_{OCP} goes down to -1.5 VSCE, demonstrating the failure of the MRP. The E_{OCP} values of PANI-HF/SAP/MRP coated sample were lower than -1.5 V_{SCE} during immersion time from 1 day to 5 days, showing the same cathodic protection time to the MRP. In the following exposure process, the E_{OCP} value of the PANI-HF/SAP/MRP sample increased due to the formation of the corrosion products around Mg particles. In the immersion time from 28 days to 210 days, the E_{OCP} values were higher than those of the MRP sample, illustrating that the protective properties of the PANI-HF/SAP/MRP sample were improved by the SAP pigments and the PANI-HF particles.

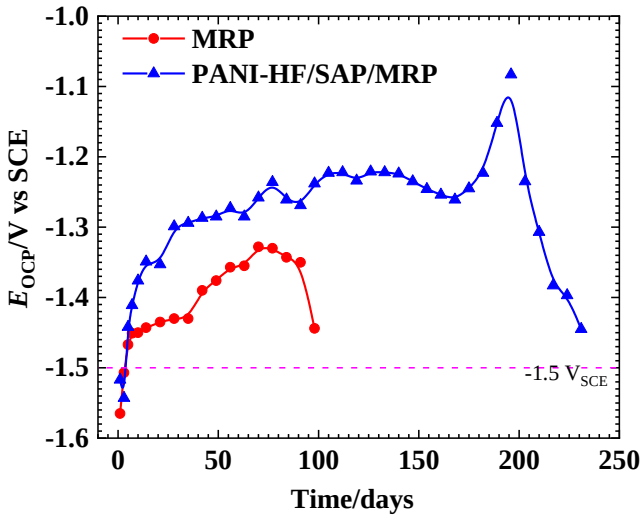

Figure 2. The changes of the OCPs for the MRP and PANI-HF/SAP/MRP coated samples with immersion time in the 3 wt% NaCl solution.

3.4. EIS measurement

Figure 3 exhibited the EIS spectra of the MRP coated samples immersed in the 3 wt% NaCl solution for various time. After 1 day of immersion, the Nyquist plot in Fig. 3a displayed a high

impedance semi-circle, and the impedance modulus value at 0.01 Hz was above 10^{10} cm^2 (Fig. 3c), indicating that the MRP had a barrier effect. After the MRP sample was immersed in the electrolyte for 3 days, the $|Z|_{0.01Hz}$ value decreased by one order of magnitude, which could be attributed to the gradual electrolyte permeation into the coating and the activation of Mg particles [9, 10, 14]. In immersion from 7 days to 28 days, a diffusion tail appeared in the Nyquist plots and the $|Z|_{0.01Hz}$ values went down obviously, reflecting that the barrier protective property of the MRP sample deteriorated gradually. Nevertheless, in immersion from 42 days to 84 days, the shape of Nyquist plots almost kept the same and the $|Z|_{0.01\ Hz}$ value decreased slowly, implying that the protective performance of the MRP remained stable without obvious deterioration. After immersion for 98 days, the Nyquist plots exhibited a tail bending to the real axis and the $|Z|_{0.01Hz}$ value was close to 10^6 Ω cm^2 (Fig. 2d), suggesting the failure of the MRP [9, 10].

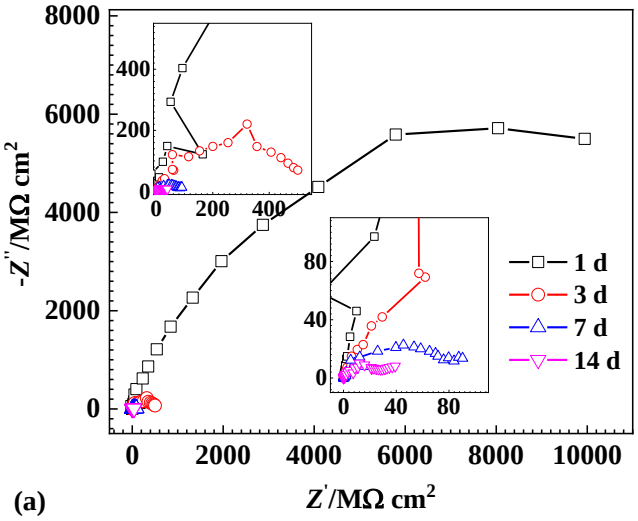

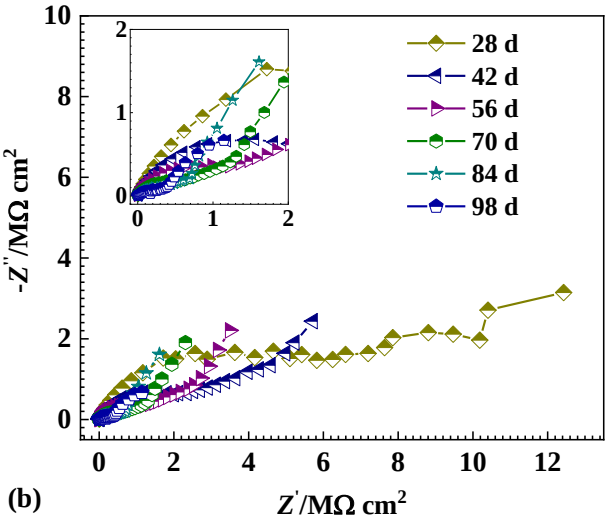

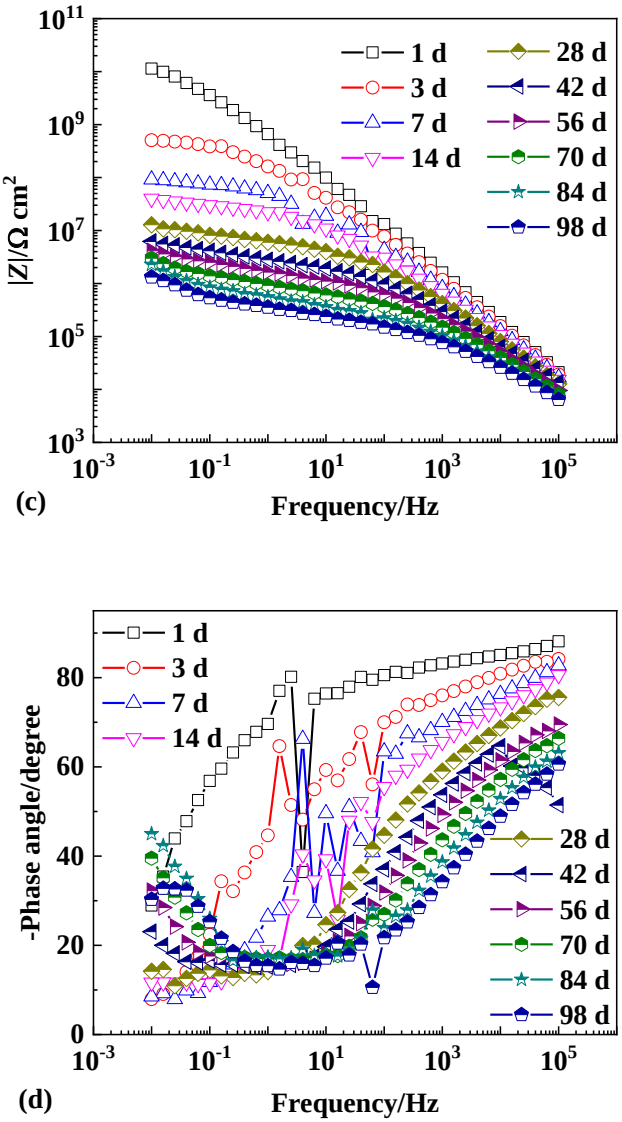

Figure 3. EIS spectra of the MRP coated samples immersed in 3 wt% NaCl solution for various time, a) and b) Nyquist plots, b) and c) Bode plots.

Figure 4 showed the EIS spectra of the PANI-HF/SAP/MRP coated samples immersed in the 3 wt% NaCl solution for various time. After 1 day of immersion, the $|Z|_{0.01Hz}$ value was higher than 10^{10} cm^2. Similar to the EIS spectra of the MRP sample, the $|Z|_{0.01Hz}$ value went down rapidly during the immersion time from 3 to 28 days because of the electrolyte permeation into the coating. Thereafter, a diffusion tail appeared in the Nyquist plots and the $|Z|_{0.01\ Hz}$ value changed slowly. However, in the immersion from 140 to 182 days, the $|Z|_{0.01\ Hz}$ value rose slightly, enhancing the barrier effect of the primer. After 231 days of immersion, the diffusion tail began to bend to the real axis and the $|Z|_{0.01\ Hz}$ value was close to 10^6 Ω cm^2 (Fig. 4d), indicating the failure of the PANI-HF/SAP/MRP [9, 10].

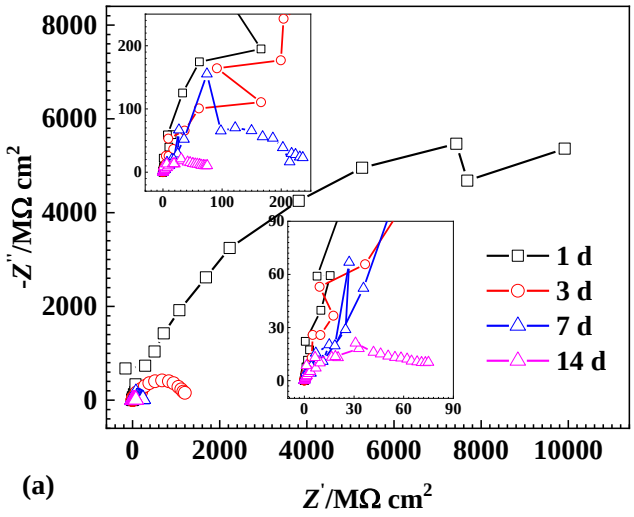
8000
6000
4000
2000
0
-Z''/MΩ cm2
0
2000
4000
6000
8000
10000
Z'/MΩ cm2
200
100
0
0
100
200
90
60
30
0
0
30
60
90
1 d
3 d
7 d
14 d

(a)

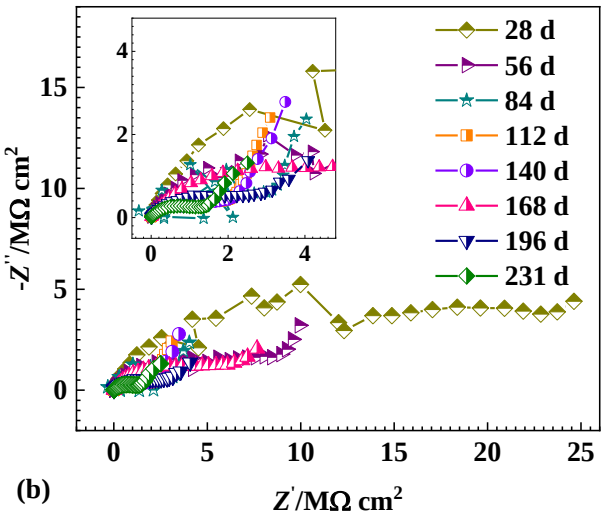
15
10
5
0
-Z''/MΩ cm2
0
5
10
15
20
25
Z'/MΩ cm2
4
2
0
0
2
4
28 d
56 d
84 d
112 d
140 d
168 d
196 d
231 d

(b)

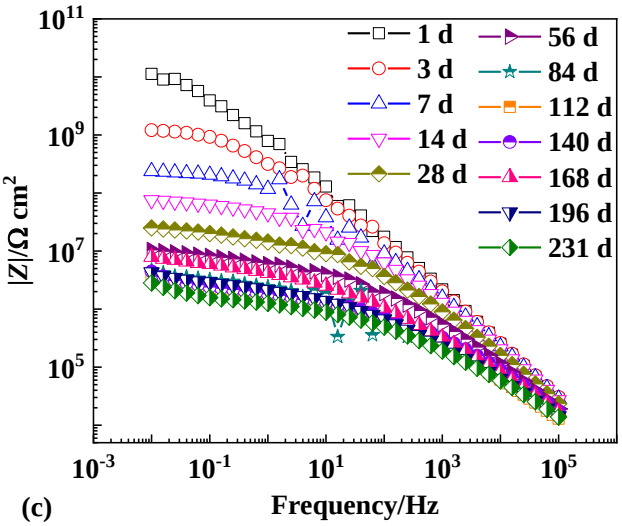
10^11
10^9
10^7
10^5
|Z|/Ω cm2
10^-3
10^-1
10^1
10^3
10^5
Frequency/Hz
1 d
3 d
7 d
14 d
28 d
56 d
84 d
112 d
140 d
168 d
196 d
231 d

(c)

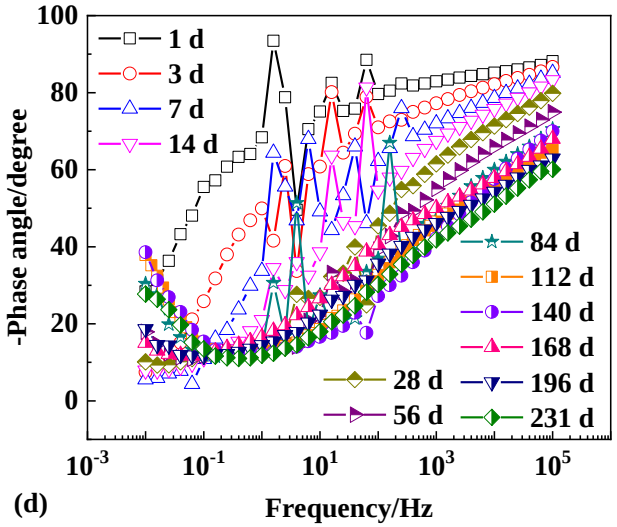

Figure 4. EIS spectra of the PANI-HF/SAP/MRPcoated samples immersed in 3 wt% NaCl solution for various time, a) and b) Nyquist plots, b) and c) Bode plots.

Figure 5 showed the variations of $|Z|_{0.01\ Hz}$ values for different coating samples in the 3 wt% NaCl solution for different time. At the beginning of immersion, the $|Z|_{0.01\ Hz}$ values of the MRP and the PANI-HF/SAP/MRP coated samples decreased remarkably due to the electrolyte permeation into the coatings and the activation of Mg particles [9, 10, 14].

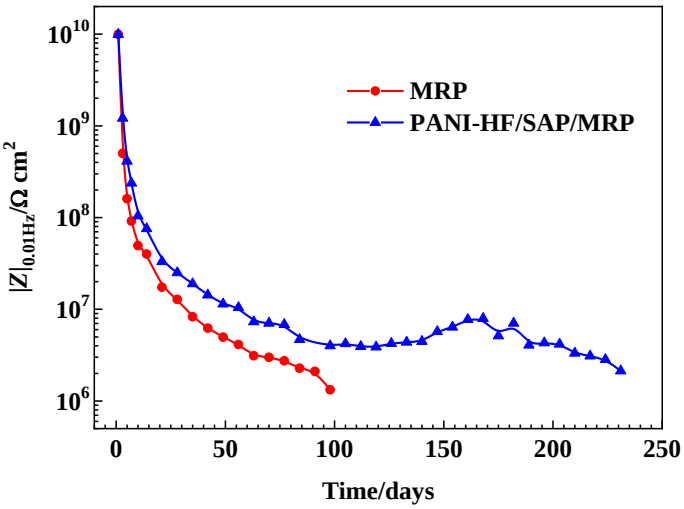

Figure 5. The variations of $|Z|_{0.01\ Hz}$ values for different coating samples in the 3 wt% NaCl solution for different time.

After immersed for 98 days, the MRP presented a $|Z|_{0.01\ Hz}$ values close to 10^6 Ω cm^2, implying the coating failure. In contrast, although the $|Z|_{0.01\ Hz}$ values the PANI-HF/SAP/MRP coated sample also slowly declined after the initial decrease, yet they showed a small rise in the immersion from 140

to 182 days. Besides, during the immersion process of 231 days, the $|Z|_{0.01\ Hz}$ values of the PANI-HF/SAP/MRP coated sample were above those of the MRP coated sample, demonstrating that the coating performance was improved by the SAP pigments and the PANI-HF particles.

Figure 6 presented the electrical equivalent circuits (EECs) adopted to fit the EIS results of the intact coatings. In order to obtain accurate results, constant phase elements (CPE), *Q*, was employed to fit the capacitive responses. The impedance of *Q* is defined as

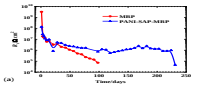

(1)

where Y_0 is the CPE constant, $j = \sqrt{-1}$, f is the frequency (Hz), $n = \alpha/(\pi/2)$, and α is the phase angle of the CPE (radians).

In the previous studies, the EECs (Fig. 6) were utilized to fit the EIS results of MRPs on AZ91D Mg alloys [9, 10, 13, 15]. Where, the physical meanings of R_c and Q_c are coating resistance and coating capacitance, respectively. R_{ct} and Q_{dl} are the charge-transfer resistance and the double layer capacitance of the Mg particles in the coatings, respectively. The corrosion products of Mg particles caused a diffusion processes in the coatings, which can be can be represented with Z_{diff}, which consists of the resistance R_{diff} in parallel to the capacitance Q_{diff} [9, 13 14, 26, 27]. When the AZ91D alloy started to corrode, the lateral diffusion of the electrolyte at the substrate/coating interface generated another time constants ($R_{sf}C_{sf}$) [28-30]. Since a film composed of the corrosion products will be formed on the substrate, R_{sf} and C_{sf} are the film resistance and film capacitance, respectively [27, 31]. Model A matched the EIS results of the MRP coated sample well in the immersion from 1 to 84 days while Model B matched well in the immersion from 91 to 98 days. For the PANI-HF/SAP/MRP coated samples, good fitting results were supplied by Model A in the immersion from 1 to 224 days while Model B after 231 days of immersion.

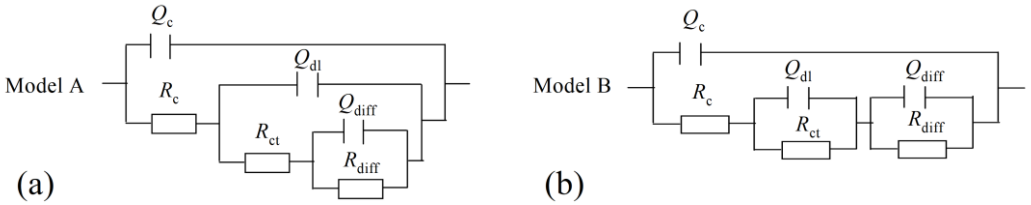

Figure 6. Equivalent electrical circuits employed to fit EIS spectra: a) stable stage, b) late stage.

Figure 7 presented the variations of R_c and R_{ct} for different coating samples. The electrolyte penetrates into coatings through pores or capillary channels, the number of which is usually represented with R_c [32, 33]. Generally, R_c declines as electrolyte permeates into coatings. As shown in Fig. 6, the R_c values of the MRP and the PANI-HF/SAP/MRP coated samples went down sharply at the beginning of the immersion, which could be attributed to the initial electrolyte penetration. After 35 days of immersion, the R_c values of the PANI-HF/SAP/MRP coated sample were higher than those of the MRP coated sample and maintained relatively stable for 196 days of immersion, suggesting that

the addition of SAP pigments and PANI-HF particles could strengthen the long-term immersion stability of the MRP.

R_{ct} is employed to represent the electrochemical reaction activity of Mg particles in the coatings and their interface stability with the binder [9, 17]. Originally, Mg particles were coated by a thin film of Mg oxide. With the electrolyte permeation into the coatings, the dissolution of magnesium oxide exposes more Mg particles to the electrolyte, resulting in the decrease of R_{ct} values. Next, the corrosion products of Mg particles precipitated in coatings, leading to an increase of the R_{ct} values for the MRP coated sample. Since micro defects in the MRP increased gradually with the immersion time, the coating contained more electrolytes, contributing to the sharp decline of R_{ct} values. In the initial immersion, the R_{ct} values of the PANI-HF/SAP/MRP coated samples decreased, attributing to the activation of the Mg particles. Nevertheless, the R_{ct} values of the PANI-HF/SAP/MRP coated samples were higher than those of the MRP sample and fluctuated above the R_{ct} values of the MRP sample. Therefore, the addition of PANI-HF particles and SAP pigments could reduce the dissolution rate of Mg particles.

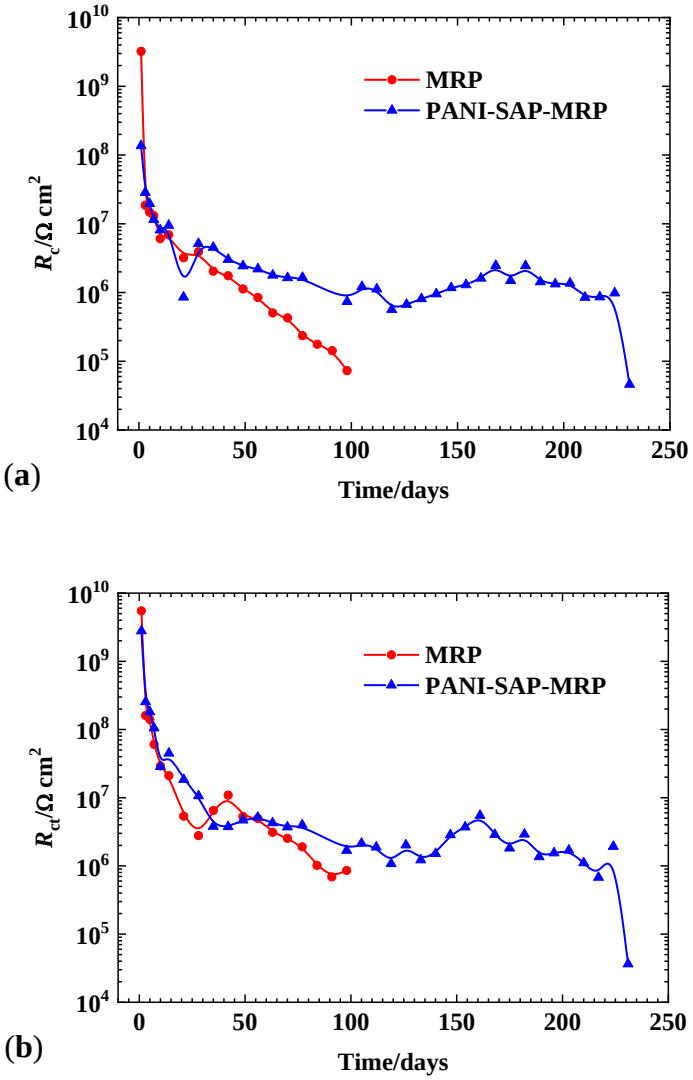

Figure 7. The variations of the fitting parameters of EIS spectra with time: (a) coating resistance, R_c; (b) charge-transfer resistance R_{ct}.

Figure 8a displayed the Nyquist plots of a sample with the defected MRP in the 3 wt% NaCl solution. After 24 hours of immersion, the Nyquist plots showed an inductive loop in the low frequency domain, indicating that severe corrosion occurred on the substrate. After 48 hours of immersion, the impedance value went up but the inductive loop still exited in the Nyquist plot, suggesting the improvement of the barrier performance on the damaged area. After 24 h of immersion SEM revealed the morphology of the scribed area and a precipitation with loose structure, $Mg(OH)_2$ [9], covered the defected area (Fig. 10).

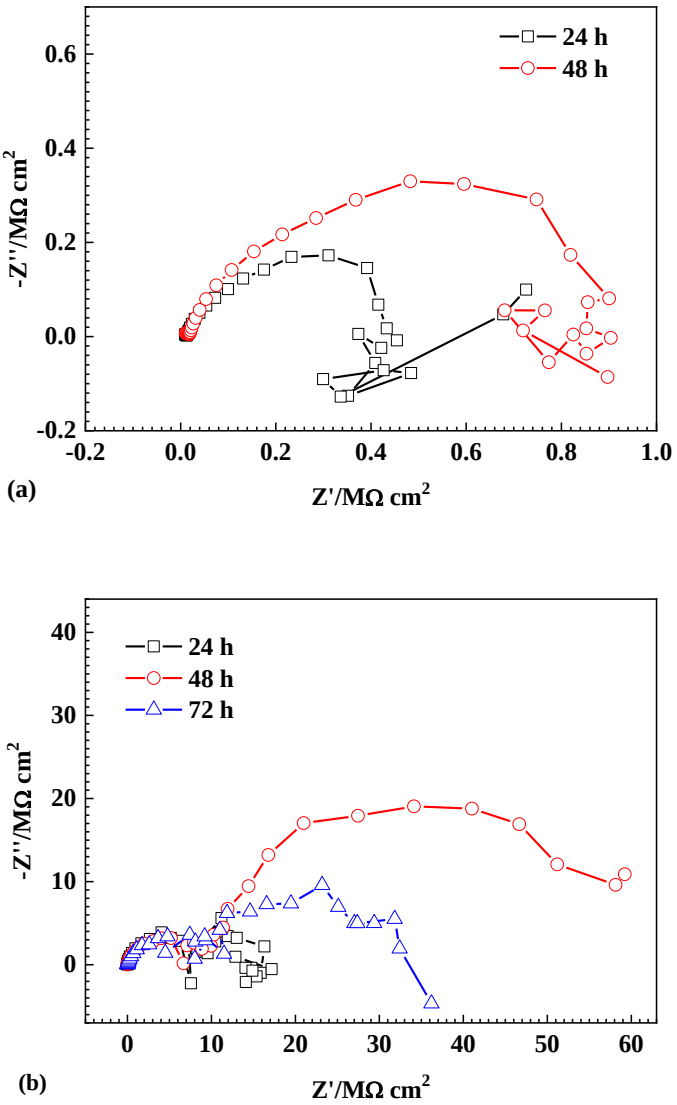

Figure 8. Nyquist plots of the samples coated with defected coatings in 3 wt% NaCl solution for different time: a) MRP and b) PANI-HF/SAP/MRP.

Figure 8b presented the Nyquist plots of the defected PANI-HF/SAP/MRP coated sample in the 3 wt% NaCl solution. The Nyquist plot shape of the sample was similar to that of the defected MRP sample after 24 hours of immersion. After 48 hours of immersion, the inductive loop disappeared, suggesting that corrosion process at the defect area was inhibited. In addition, the impedance value went up, reflecting that the barrier performance on the defected area was enhanced to some extent.

After 72 hours of immersion, the impedance value declined, indicating a deterioration of the barrier property on the defected area, but still higher than that of the defected MRP sample. The morphology of the defected area after 72 hours of immersion was observed by SEM and showed that the corrosion products existed on the defected area (Fig. 9d). The corrosion product structure of the PANI-HF/SAP/MRP was more compact than that of the MRP, suggesting that the SAP pigments and the PANI-HF particles improved the protective performance on the defected coating.

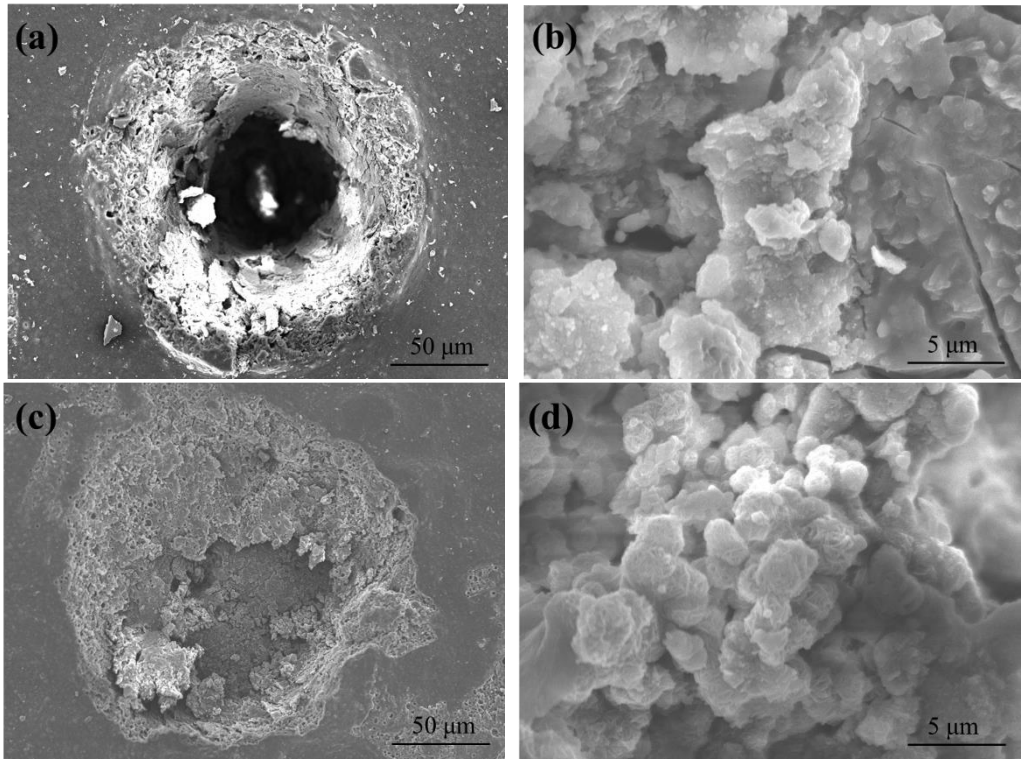

Figure 9. The morphology of the defected areas on different coatings: a) and b) MRP; c) and d) PANI-HF/SAP/MRP.

3.5 Substrate analysis

Figure 10 displayed the surface morphologies of the AZ91D alloy substrates underneath the MRP and the PANI-HF/SAP/MRP after different immersion time in the 3 wt% NaCl electrolyte. After 98 days of immersion, the AZ91D alloy underneath the MRP was covered by the film with a loose structure (Fig. 10a). The film consisted mainly of $Mg(OH)_2$ and MgO, and was about a few nanometers thick [14, 34]. For the PANI-HF/SAP/MRP coated sample, the underneath AZ91D alloy presented a relatively compact layer (Fig. 10b).

In order to analyze the chemical compositions of the film in Fig. 10b, XPS was carried out on the substrate underneath the PANI-HF/SAP/MRP after immersion for 231 days in the 3 wt% NaCl solution. The P $2p_{3/2}$ peak in Fig.10a corresponded to the SAP pigment [14], indicating that phosphates existed in the film. The O 1s spectra in Fig. 11b revealed four main peaks at 531.1 eV, 531.6 eV, 532.1

eV and 532.8 eV arising from the MgO [35], O/(-C_6H_5-N-H-)$_n$ [25], $Mg(OH)_2$ [35] and metaphosphate (P-O-P, P-O-Mg) [35, 36]. The Mg 1s spectrum (Fig. 10c) consisted of three peaks with binding energy of 1302.8 eV, 1303.7 eV and 1304.7 eV, respectively attributing to Mg in AZ91D matrix [37], and the magnesium oxides [38] and Mg-PO_y in the film [14]. The above results demonstrated the film on the substrate underneath the PANI-HF/SAP/MRP was mainly composed of magnesium oxides and phosphates. The XPS spectra of a bare AZ91D alloy before exposure were analyzed in our previous study [14]. In contrast, $Mg(OH)_2$ and MgO were the main chemical compositions of the film on the bare AZ91D alloy [14]. Therefore, the addition of the SAP pigments generated Mg phosphate in the film, which improved the layer compactness.

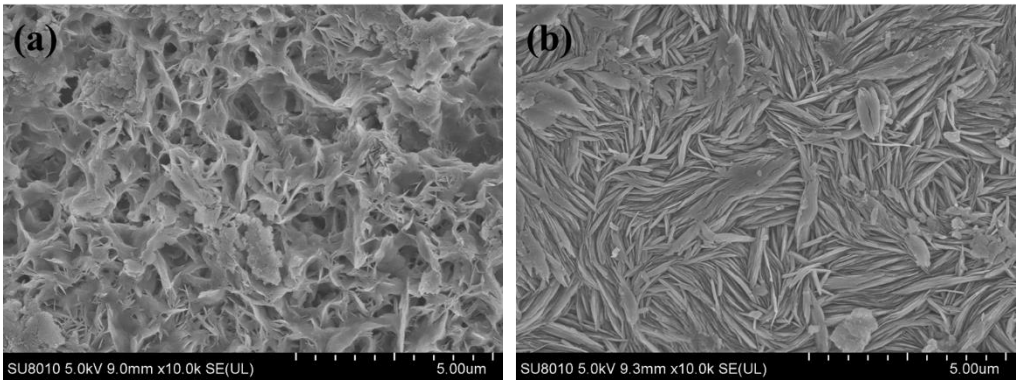

Figure 10. SEM morphologies of the AZ91D alloy underneath MRP after immersion for 98 days (a) and the substrate surfaces underneath PANI-HF/SAP/MRP after immersion for 231 days (b).

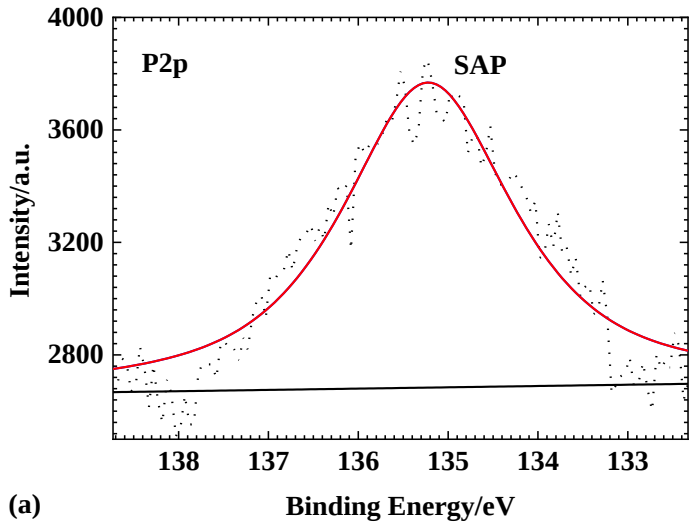

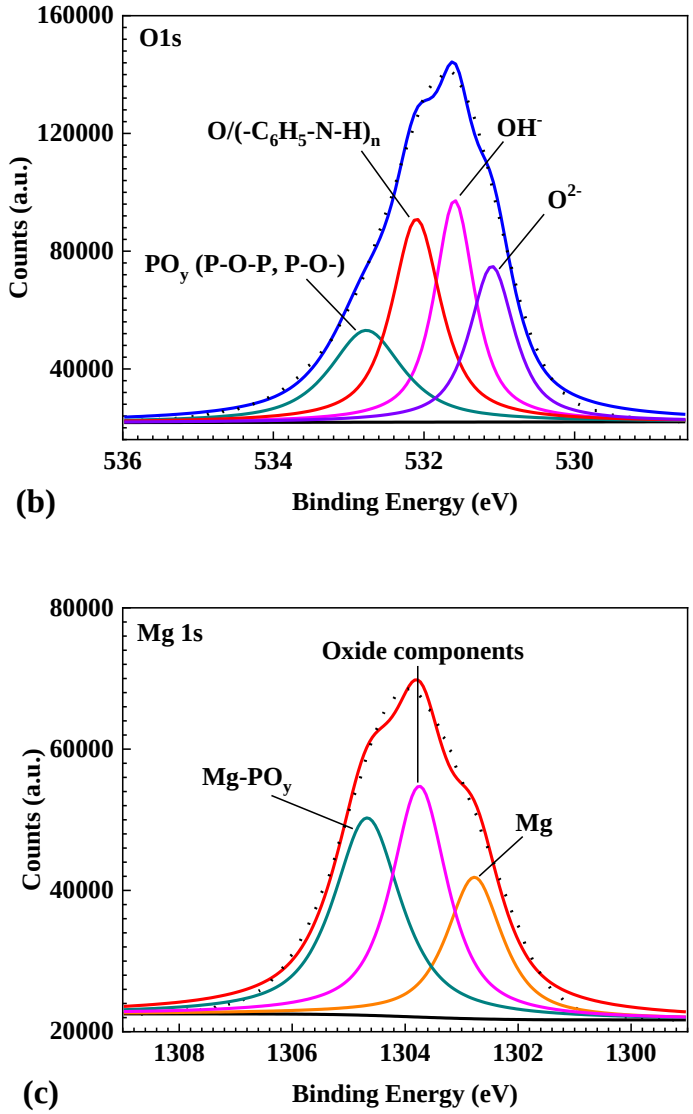

Figure 11. XPS spectra on the substrate surface underneath PANI-HF/SAP/MRP after 231 days of immersion in the 3 wt% NaCl solution: (a) P2p, (b) O1s and (c) Mg1s.

3.6. Discussion

When PANI-HF particles and SAP pigments were both added in the MRP, the OCP results showed that the cathodic protection time of the MRP and the PANI-HF/SAP/MRP for AZ91D alloy were both 5days (Fig. 2), suggesting that the cathodic protection time was not enhanced by PANI-HF particles and SAP pigments. For the PANI-HF/SAP/MRP, the electric connection bridge of PANI-HF particles for Mg particles disappeared due to the relatively low levels of the Mg-particle loading [25]. The SAP pigments did not slow down the rapid passivation of Mg particles in the presence of PANI-HF particles. However, PANI-HF particles and SAP pigments significantly improved the barrier effect of the MRP in the long immersion, proved by the variations of $|Z|_{0.01\ Hz}$ (Fig. 5), R_c (Fig. 7a) and R_{ct} (Fig. 7b) values. SEM observation (Fig. 10) and XPS (Fig. 11) analysis of the AZ91D alloy underneath

the PANI-HF/SAP/MRP presented that a protective layer, consisting of Mg oxides and phosphates, deposited on the substrate. It could be deduced that the corrosion products of Mg particles in the PANI-HF/SAP/MRP were mainly composed of Mg oxides and phosphates and enhanced the coating barrier effect. That conclusion could be demonstrated by the increase of $|Z|_{0.01\ Hz}$ (Fig. 5), R_c (Fig. 7a) and R_{ct} (Fig. 7b) values. In addition, the characterization of the defected PANI-HF/SAP/MRP (Fig. 8b and Fig. 9c) indicated that the corrosion products of Mg particles in the PANI-HF/SAP/MRP were relatively dense and could heal the micro defects in the coating. The single addition of PANI-HF particles o SAP pigments increased the service life of MRP by 1.3 times [25] and 2 times [14], respectively. Nevertheless, the combined addition of PANI-HF particles and SAP pigments increased the MRP life by 2.4 times, indicating that PANI-HF particles and SAP pigments can play a good synergistic effect in improving the MRP performance. Above all, the PANI-HF particles and the SAP pigments could make the corrosion products of Mg particles compact to improve the MRP stability and generate a protective layer on the AZ91D alloy to retard its corrosion.

4. CONCLUSIONS

(1)The protective performance of the MRP was improved with the addition of PANI-HF particles and SAP pigments. Machu test results showed that the PANI-HF/SAP/MRP provided better protection for the AZ91D alloy at the coating defect than the MRP.

(2) The characterization of the defected PANI-HF/SAP/MRP indicated that the corrosion products of Mg particles in the coating were relatively dense and could heal the coating micro defects. XPS results indicated that a protective layer composed of Mg oxides and phosphates was formed on the AZ91D substrate beneath the PANI-HF/SAP/MRP.

(3) The improvement mechanism of the PANI-HF particles and the SAP pigments to the MRP was illustrated as follows. The barrier effects of the MRP were enhanced by the precipitation of the corrosion products, Mg oxides and phosphates, around Mg particles. In addition, a protective layer on the AZ91D substrate underneath the PANI-HF/SAP/MRP retarded the corrosion of the substrate.

ACKNOWLEDGMENTS
This work is supported by the Fundamental Research Funds for the Central Universities (B200202060) and the Open Project supported by State Key Laboratory for Marine Coatings (GZS-001-2020).

References

1. Z. Zeng, N. Stanford, C.H.J. Davies, J.-F. Nie, N. Birbilis, *Int. Materials Reviews*, 64 (2019) 27.
2. S. You, Y. Huang, K. Kainer, N. Hort, *J. Magnes. Alloy.*, 5 (2017) 239.
3. M. Esmaily, J.E. Svensson, S. Fajardo, N. Birbilis, G.S. Frankel, S. Virtanen, R. Arrabal, S. Thomas, L.G. Johansson, *Prog. Mater. Sci.*, 89 (2017) 92.
4. Y. Li, X. Lu, K. Wu, L. Yang, T. Zhang, F. Wang, *Corros. Sci.*, 168 (2020) 108559.
5. X. Lu, J. Hu, Y. Zhao, M. Wang, X. Wang, Z. Ye, Z. Zheng, J. Hu, X. Feng, *J. Electrochem. Soc.*, 168 (2021) 080513.

6. H. Wei, Y. Wang, J. Guo, N.Z. Shen, D. Jiang, X. Zhang, J. Zhu, Q. Wang, L. Shao, H. Lin, S. Wei, Z. Guo, *J. Mater. Chem. A*, 3 (2015) 469.
7. A.S. Gnedenkov, S.L. Sinebryukhov, D.V. Mashtalyar, S.V Gnedenkov, *Corros. Sci.*, 102 (2016) 348.
8. S.G.R. Emd, S. Morsch, T. Hashimoto, Y. Liu, S.R. Gibbon, S.B. Lyon, X. Zhou, *Pro. Org. Coat.*, 137 (2019) 105340.
9. X. Lu, Y. Zuo, X. Zhao, Y. Tang, X. Feng, *Corros. Sci.*, 53 (2011) 153.
10. X. Lu, Y. Zuo, X. Zhao, S. Shen, *Int. J. Electrochem. Sci.*, 10 (2015) 9586.
11. G.L. Song, N.J. Dudney, J. Li, R.L. Sacci, J.K. Thomson, *Corros. Sci.*, 87 (2014) 11.
12. G.L. Song, A. Atrens, M. Dargusch, *Corros. Sci.*, 41 (1999) 249.
13. X. Lu, Y. Zuo, X. Zhao, Y. Tang, *Corros. Sci.*, 60 (2012) 165.
14. X. Lu, Y. Zuo, X. Zhao, Y. Tang, *Electrochim. Acta*, 93 (2013) 53.
15. X. Lu, X. Feng, Y. Zuo, C. Zheng, S. Lu, L. Xu, *Surf. Coat. Technol.*, 270 (2015) 227.
16. X. Lu, X. Feng, Y. Zuo, P. Zhang, C. Zheng, *Prog. Org. Coat.*, 104 (2017) 188.
17. D. Battocchi, A. M. Simões, D. E. Tallman, G. P. Bierwagen, *Corros. Sci.*, 48 (2006) 1292.
18. J.R. Vilche, E.C. Bucharsky, C.A. Giúdice, *Corros. Sci.*, 44 (2002) 1287.
19. S. S. Pathak, M. D. Blanton, S. K. Mendon, J. W. Rawlins, *Corros. Sci.*, 52 (2010) 3782.
20. J. Wang, Y. Zuo, Y. Tang, X. Lu, *Appl. Surf. Sci.*, 292 (2014) 93.
21. P. Xu, X. Lu, H. Cheng, X. Feng, Z. Zhao, Y. Ding, Y. Shen, X. Shi, *Prog. Org. Coat.*, 135 (2019) 591.
22. X. Lu, S. Sun, Q. Fan, X. Pei, Y. Dun, X. Feng, C. Zou, W. Lu, *Coatings*, 9 (2019) 649.
23. S. Shen, Y. Zuo, X. Zhao, *Corros. Sci.*, 76 (2013) 275.
24. S. Shen, Y. Zuo, *Corros. Sci.*, 87 (2014) 167.
25. X. Feng, C. Zhu, X. Lu, Y. Zhang, T. Wu, Y. Zuo, X. Zhao, Y. Dun, M. Wang, *Prog. Org. Coat.*, 141 (2020) 105550.
26. H. Marchebois, M. Keddam, C. Savall, J. Bernard, S. Touzain, *Electrochim. Acta*, 49 (2004) 1719.
27. J.T. Zhang, J.M. Hu, J.Q. Zhang, C.N. Cao, *Prog. Org. Coat.*, 51 (2004) 145.
28. C. Gabrielli, M. Keddam, O.R. Mattos, H. Takenouti, *J. Electroanal. Chem. Interfacial Electrochem.*, 117 (1981) 147.
29. C. I. Elsner, E. Cavalcanti, O. Ferraz, A. R. Di Sarli, *Prog. Org. Coat.*, 48 (2003) 50.
30. B. del Amo, L. Véleva, A. R. Di Sarli, C.I. Elsner, *Prog. Org. Coat.*, 50 (2004) 179.
31. J. M. Hu, J. Q. Zhang, C. N. Cao, *Prog. Org. Coat.*, 46 (2003) 273.
32. M. Kendig, F. Mansfeld, S. Tsai, *Corros. Sci.*, 23 (1983) 317.
33. H. Liu, F. Cao, G.-L. Song, D. Zheng, Z. Shi, M.S. Dargusch, A. Atrens, *J. Mater. Sci. Technol.*, 35 (2019) 2003.
34. N.S. Mcintyre, C. Chen, *Corros. Sci.*, 40 (1998) 1697.
35. M. Santamaria, F. Di Quarto, S. Zanna, P. Marcus, *Electrochim. Acta*, 53 (2007) 1314.
36. H. Ardelean, I. Frateur, S. Zanna, A. Atrens, Marcus, P. *Corros. Sci.*, 51 (2009) 3030.
37. W. He, E. Zhang, K .Yang, *Mat. Sci. Eng. C-Mater.*, 30 (2010) 167.
38. C. Wang, S. Zhu, F. Jiang, F. Wang, *Corros. Sci.*, 51 (2009) 2916.